



SCRIPTING CARTOGRAPHIC METHODS OF GMT FOR MAPPING THE NEW BRITAIN AND SAN CRISTOBAL TRENCHES, SOLOMON SEA, PAPUA NEW GUINEA

MÉTODOS CARTOGRÁFICOS DE SCRIPT DE GMT PARA MAPEAR AS TRINCHEIRAS DA NOVA GRÃ-BRETANHA E SAN CRISTOBAL, MAR DE SALOMÃO, PAPUA-NOVA GUINÉ

 <https://doi.org/10.35701/rcgs.v22n3.717>

Polina Lemenkova¹

Histórico do Artigo:

Recebido em 09 de Novembro de 2020

Aceito em 09 de Dezembro de 2020

Publicado em 30 de Dezembro de 2020

ABSTRACT

The study present a case study of the Generic Mapping Tools (GMT) applied for cartographic modelling, mapping and comparative analysis of the deep-sea trenches located in southwest Pacific Ocean: the New Britain Trench (NBT) and the San Cristobal Trench (SCT). The aim was to evaluate their geomorphic variation using scripting cartographic approach of GMT. The data was processed using a sequence of the GMT modules with the main module 'grdtrack' used to visualize cross-section profiles along the trenches for their geomorphological modelling. The main grid used for topographic mapping is the SRTM DEM with 15-arc second resolution. The statistical analysis shown variability in depths of both trenches by samples in two transects. The cartographic analysis demonstrated following results. The SCT is generally deeper reaching -9,000 m, while the median for the NBT less then 7,000 m. The gradient slope of SCT is more symmetric with accurate 'V' form. In a cross-section graph, the NBT landward slope is markedly asymmetric U-shaped form and has a crescent form in the east. The NBT slope dips westwards with 35° eastward, and 41° westward, while the SCT slope has 33° oceanwards and 33,69° landwards. The difference between the geomorphology of the trenches is explained by the effects of the geotectonic evolution and actual sedimentary processes affected their formation and sculptured their structure. The marine free-air gravity anomaly illustrated density anomalies at the bathymetry in the region of NBT and SCT with range <-60.0 mGal. The geoid values are 56-66 mGal. The study contributed to the submarine geomorphic mapping and presents technical application of the cartographic functionality of GMT used for geomorphological modelling.

Keywords: GMT, Cartography, SRTM, San Cristobal Trench, New Britain Trench.

¹ Senior Engineer at Schmidt Institute of Physics of the Earth, Russian Academy of Sciences. Department of Natural Disasters, Anthropogenic Hazards and Seismicity of the Earth. Laboratory of Regional Geophysics and Natural Disasters (Nr. 303). Bolshaya Gruzinskaya St, 10, Bld. 1, Moscow, 123995, Russian Federation. Tel.: +7-916-298-37-19. Email: pauline.lemenkova@gmail.com,

 <https://orcid.org/0000-0002-5759-1089>

RESUMO

O estudo apresenta um estudo de caso de Ferramentas de Mapeamento Genéricas (GMT) para modelagem cartográfica, mapeamento e análise comparativa das trincheiras de alto mar localizadas no sudoeste do Oceano Pacífico: a New Britain Trench (NBT) e a San Cristobal Trench (SCT). O objetivo foi avaliar sua variação geomórfica utilizando abordagem cartográfica de script de GMT. Os dados foram processados usando uma sequência de módulos GMT com o módulo principal 'grdtrack' usado para visualizar perfis de seção transversal ao longo das trincheiras para sua modelagem geomorfológica. A grade principal usada para mapeamento topográfico é o SRTM DEM com resolução de 15 segundos de arco. A análise estatística mostrou variabilidade nas profundidades de ambas as trincheiras por amostras em dois transectos. A análise cartográfica demonstrou os seguintes resultados. O SCT é geralmente mais profundo atingindo -9.000 m, enquanto a mediana para o NBT é inferior a 7.000 m. O declive do gradiente de SCT é mais simétrico com forma em 'V' precisa. Em um gráfico de seção transversal, a inclinação NBT em direção à terra é marcadamente assimétrica em forma de U e tem uma forma crescente no leste. A encosta NBT mergulha para oeste com 35 ° para leste e 41 ° para oeste, enquanto a encosta SCT tem 33 ° para o mar e 33,69 ° para terra. A diferença entre a geomorfologia das trincheiras é explicada pelos efeitos da evolução geotectônica e os processos sedimentares reais afetaram sua formação e esculpiram sua estrutura. A anomalia da gravidade marítima ao ar livre ilustrou anomalias de densidade na batimetria na região de NBT e SCT com intervalo <-60,0 mGal. Os valores do geóide são 56-66 mGal. O estudo contribuiu para o mapeamento geomórfico submarino e apresenta aplicação técnica da funcionalidade cartográfica do GMT utilizada para a modelagem geomorfológica.

Palavras-chave: GMT. Cartografia. SRTM. San Cristobal Trench. New Britain Trench.

INTRODUCTION

Selecting the best cartographic GIS software is a topic that attracts attention and gaining importance nowadays with a wide variety of existing GIS. The functionality of GIS software for cartographic plotting, mapping and graphical visualization in a geospatial research can affect the workflow and result in different map layouts. The available GIS presents a wide variety of geoinformation software, which can be listed to mention a few of the most well-known ones: ArcGIS, QGIS, ENVI GIS, GRASS GIS, Erdas Imagine, SAGA GIS, Idrisi GIS, MapInfo, GeoMedia. In view of this, there is a need to know the advantages and functionality of the possible GIS software and tools that can be applied for the research and mapping.

The Generic Mapping Tools (GMT) stands apart from the traditional GIS due to its highly specific functionality consisting of a console and a scripting approach, without Graphical User Interface (GUI) with a menu. The basis for mapping workflow in GMT is writing a script consisting form several lines of code taken together as a script for plotting maps. This can be achieved by a console and traditional scripting development environment (e.g. Xcode, Atom). The functionality of GMT enables its excellent operating of the cartographic commands which results in a high flexibility of writing a code and executing a script stepwise with a full control on the cartographic output. Many studies on mapping and spatial analysis are based on testing different GIS applied for various research questions, in which a large number of articles reported either the cartographic workflow and techniques of visualization (ČESNULEVIČIUS et al. 2019; KESKIN et al. 2019; LÓPEZ & BALBOA 2008; WOOD, 1993;

LEMENKOVA, 2019a, 2019b, 2020a; BIEDA et al. 2020), present analysis of the cartographic visualization (e.g. OSTROWSKI et al. 2019; MESENBUR, 2004; KEATES, 1996) or focused on the technical GIS applications (MACEACHREN, 1995; SLOCUM et al. 1993; ROBINSON et al. 1995). GOMARASCA (2009) points that cartographic visualization and mapping are of fundamental importance for the geospatial data.

Indeed, the effectively plotted and precise maps can serve as excellent tools for indicating the relationship between the geographic phenomena of the Earth, help to focus on the correlations between the geological and geophysical processes, to elements of the geological structures and highlight the complexity of the geospatial systems. The study conducted by DENT (1999) showed a high level of importance concerning the mapping workflow which includes the map projections, map design, and map production, since the quality of the layout maps impacts the quality of the data analysis. In various research papers on cartography (YOELI, 1983; TYNER, 1992; TOBLER, 1974), the methodology approaches in spatial analysis and mapping workflow are highlighted as important cartographic issues.

This study presents a GMT as a main cartographic toolset for modelling geomorphological profile of the two deep-sea trenches, and visualization the geological and geophysical settings as indication of impact of the tectonic development on the actual landform of the seafloor. Not all the GIS are equally functional and enable to perform a complex cartographic analysis based on the machine learning. In contrast with traditional GIS, the majority of which use GUI, the GMT uses scripting, which presents a high degree of automatization and repeatability in the cartographic workflow. For example, the GMT based cartographic techniques used in this research, included the following major steps: visualization of the image using the 'grdimage' module; plotting the isolines using the 'grdcontour'; inserting the global small map for identification of the study area location in a topographic map; annotating the texts and inserting legend; adding cartographic elements by 'psbasemap' module; automatic digitizing of the cross-section profiles for a spatial geomorphological analysis; calculation of the data frequency in histogram of depths distribution by the 'pshistogram' module; modelling the curvature trends for geomorphological analysis of steepness of the slopes by 'trend1d' module; as well as visualizing various raster grids (EGM2008, SRTM) within the investigated area.

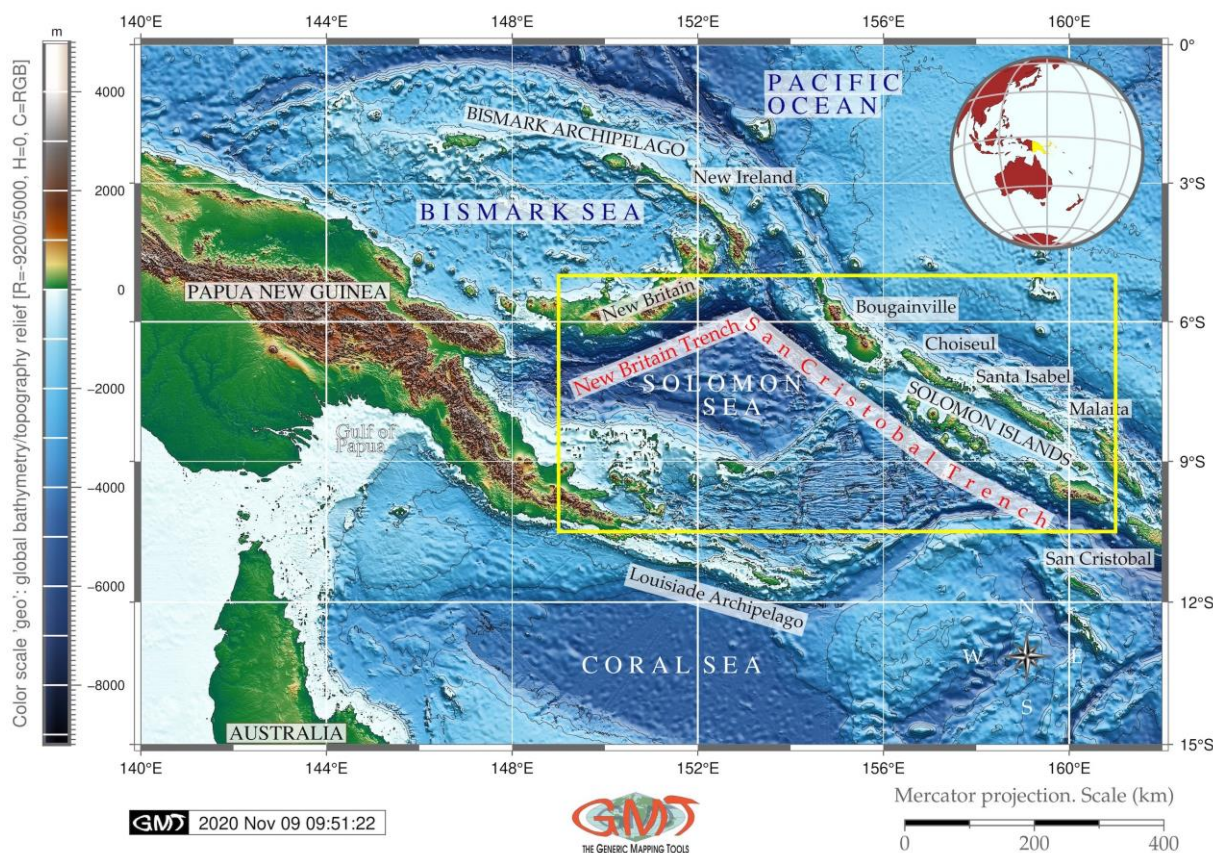
The aim of this study was to present the results of the application of GMT for geophysical and geological data visualization and geomorphological modelling in one of the marginal seas of the Pacific Ocean: the Solomon Sea with the two deep-sea trenches, the New Britain Trench and the San Cristobal Trench. The study objective is to contribute to the knowledge on deep-sea trench geomorphology in the Pacific Ocean region, perform cartographic visualization of the geophysical and geological settings

around the New Guinea and northern Australia region and present modelling of hadal geomorphology using GMT.

Study area

The study area is focused on the New Britain and San Cristobal hadal trenches located eastwards off Papua New Guinea as northern borders of the Solomon Sea, Pacific Ocean (Fig. 1). The region is one of the world's active subduction zones at the triple junction of the Pacific Plate, Indo-Australian Plate and Solomon Sea Plate. Additionally, the Woodlark Basin subducts beneath the Solomon Islands arc region, forming a double-sided subduction zone (YONESHIMA et al., 2005). Because the region is situated within the complex zone of the convergence at the tectonic plates boundary, it is trapped between the converging Ontong Java Plateau and Australian continent. Geologically, the study area belongs to one of the most prospective for intrusion-related mineral deposits (HOLM et al., 2019).

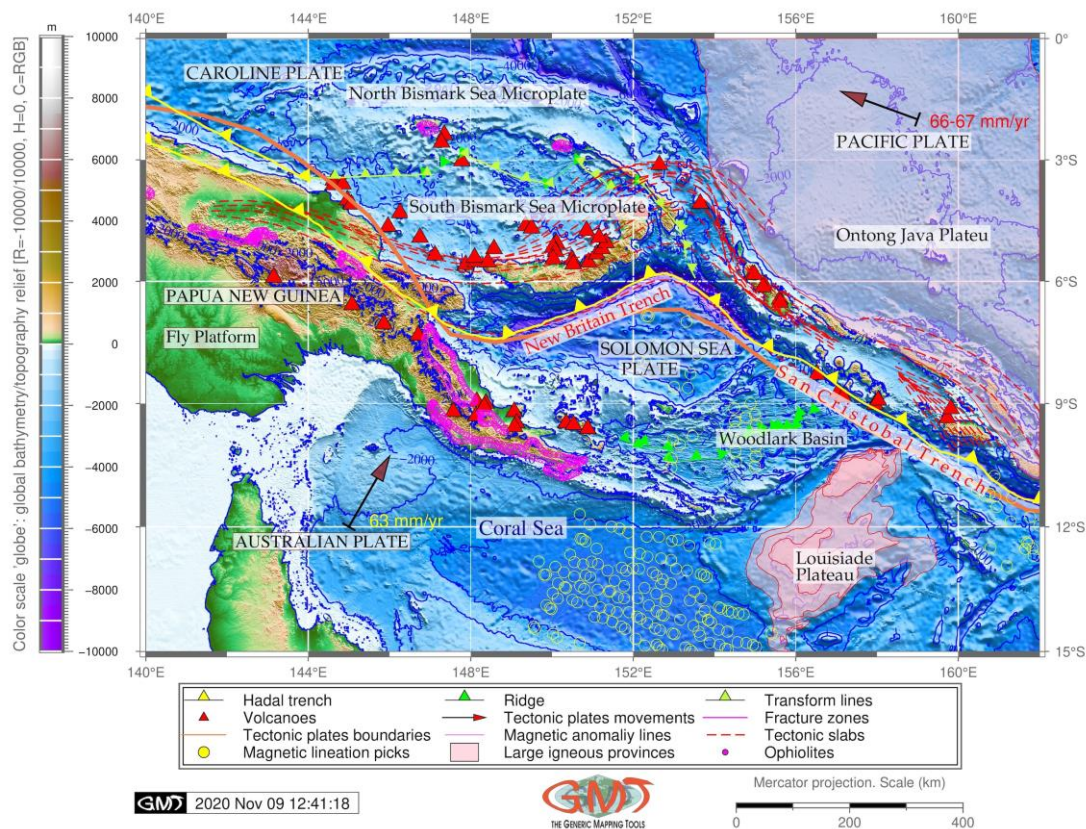
Figure 1: Topographic map of the New Britain and San Cristobal trenches. SRTM Global Relief Model 15 arc sec.



Source: Author (2020).

The New Britain Trench (a.k.a. Bougainville Trench) is defined by the 6,000 m isoline. It is a narrow, 50-75 km wide trench extending northeasterly from the eastern end of the Huon Gulf along the south coast of New Britain (MAMMERICKX et al., 1971). Its name is derived from the homonymous New Britain Island from the New Britain arc (Fig. 2). Its western extension are the north-dipping Ramu-Markham fault zone and the West Bismarck arc (ABBOT et al., 1994). The northern part is characterized by the Bismarck Sea back-arc basin (Fig. 2) where active rifting and seafloor spreading take place. The Bismarck Sea back-arc basin comprises the South and North Bismarck microplates separated by the Bismarck Sea fault (TAYLOR, 1979). The islands of eastern Papua New Guinea and the Solomon Islands are island arc terranes, surrounding New Britain Trench, are formed adjacent to the boundary between the Australian and Pacific plates (BALDWIN et al., 2012). As pointed by LINDLEY (2006), the subduction along the New Britain Trench is crucial for the tectonic development in New Guinea because comparing to other trenches of the Pacific Ocean, the New Britain Trench differs in its seismic structure below the trench. Thus, it indicates a steeply dipping ($>80^\circ$) structure to upper mantle depths (630 km), unlike other Pacific trenches where dips range between 45° - 60° . Further discussion on New Britain Trench tectonics and structure exist in further works (WEIBENGA, 1973; AUZENDE et al., 1994).

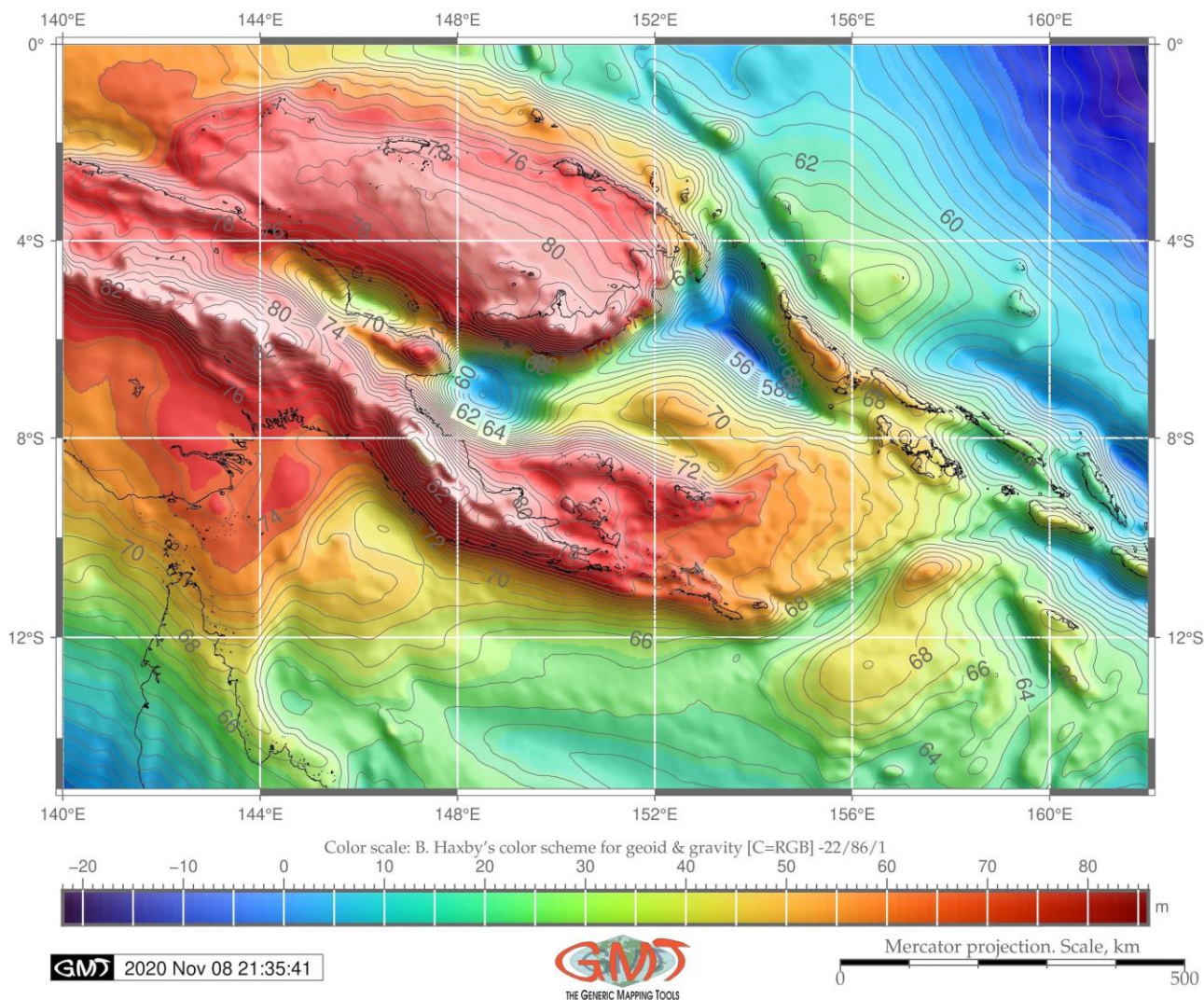
Figure 2: Geologic map of the New Britain and San Cristobal trenches, base map: SRTM.



Source: Author (2020).

The San Cristobal Trench stretches in SE direction from the junction from the New Britain along the group of Solomon Islands Bougainville, Choiseul, Santa Isabel, Malaita until it reaches San Cristobal Island from which it derived the name. The Woodlark Basin is adjacent to the San Cristobal Trench to the southwest and to the south of the Solomon Islands arc region (Fig. 2). It is a young (~5 Ma) oceanic basin that subducts beneath the New Britain Trench (YONESHIMA et al., 2005). The eastern part of the Solomon Plate bordering the San Cristobal Trench, enters the front of the Pacific Plate. As a consequence, it results of significant earthquakes along the Solomon Plate (YANG et al., 2018).

Figure 3: Geoid model: New Britain and San Cristobal trenches. EGM-2008 WGS84, 2,5 min resolution.



Source: Author (2020).

The active volcanic arc that can be seen along the north coast of New Britain Island (Fig. 2, red triangles) correlates with subduction curve along the New Britain Trench. The environment of the hadal trench presents a complex system with highly interconnected factors affecting geomorphological

structure, formation and development of the trench: slabs and tectonics plates, bathymetry, geographic location, geologic structure of the underlying basement and sediment thickness (LEMENKOVA, 2018a). Further detailed explanation on structure and these factors can be found in existing literature (DAVIES et al. 1987; FINLAYSON; CULL, 1973; TREGONING, et al., 1998; JOHNSON, 1976; LINDLEY, 1988; RIPPER, 1970; HONZA, et al., 1987) describing bathymetry, geomorphology, sedimentation, submarine canyons and terraces of the New Britain Trench. However, these works are mainly restricted to the western part of the Solomon Sea and are based on the existing data at that time. Current study proposes a comparative analysis of the New Britain Trench with its contiguous San Cristobal Trench. Moreover, this study is supported by modern datasets (SRTM 15 sec DEM, gravity and geoid grids) using fine cartographic toolset GMT.

MATERIALS AND METHODS

The methodology of the current work is completely based on using the Generic Mapping Tools (GMT) developed by WESSEL and SMITH (1998) and maintained up to date by the group of developers (WESSEL et al. 2013). The used version of the GMT is 5.4.5. Technically, the GMT based mapping and modelling is done using following major GMT modules: `grdimage` (this module visualizes raster image on the computer display, i.e. makes a physical appearance of map). The coastline contours and polygons of continents were added using existing geographic dataset in GMT (WESSEL; SMITH, 1996) by option '`pscoast`'.

Other GMT modules were used for plotting diverse cartographic elements, e.g. colour palettes (`makecpt`), adding scale (`psscale`) and data conversion to TIFF/JPG (`psconvert`), plotting isolines and contour lines (`grdcontour`), mapping basic map elements (`psbasemap`), adding GMT logo (`logo`), addition map annotations and text elements (`pstext`), plotting various vector elements, such as lines, points and polygons (`psxy`), selecting study area (`grdcut`), modelling cross-section profiles (`grdtrack` and `convert`). Besides native GMT modules, several Unix programs were used for auxiliary operating with files and texting on the maps: `echo`, `rm`, `cat`.

Data and materials: SRTM DEM

The accuracy of digital bathymetric data is essential for modelling and cartographic mapping, because input data finally determines the output results (Smith, 1993). Therefore, the data used as a main base grid in this work is a high-resolution raster Shuttle Radar Topographic Mission (SRTM) DEM, (BECKER, et al. 2009; GESCH et al., 2006b). The high-resolution topographic data generated from NASA's SRTM builds a suite of gridded raster tiles based on Earth observation survey and quality

control (GESCH, et al., 2006a). The data are available through the USGS EROS Data Center Earth Resources Observation and Science (EROS) Center. The comprehensive quality of the DEMs derived by SRTM is well evaluated (e.g. Zhang, K. et al. 2019). There are multiple applications of SRTM in geosciences due to the high quality of the grids (KOCH et al., 2002; KULP; STRAUSS, 2018; PHAM et al., 2018). The gridded topographic data of the Solomon Sea obtained from the SRTM with a resolution of roughly 15 sec highlights the bathymetry (Fig. 1) through selected 'geo' colour palette. It shows complex bathymetric patterns southwest off the San Cristobal Trench (Fig. 5).

Modelling geoid and gravity

Modelling geoid was done using a combination of GMT codes by methods described in Wessel, and Smith (2018). The GMT codes used for mapping free-air gravity are below (Table 1):

Table 1: Sequence of codes by GMT modules for gravity modelling.

Step	Purpose of code	GMT code using various modules
1	Generating a file	ps=Grav_NBT.ps
2	Extracting subset of img file	img2grd grav_27.1.img -R140/162/-15/0 -Ggrav.grd -T1 -I1 -E -S0.1 -V
3	Colour palette table (cpt) from grid	gmt grd2cpt grav.grd -Crainbow > grav.cpt
4	Generating gravity image with shading	gmt grdimage grav.grd -I+a45+nt1 -R140/162/-15/0 -JM16c -Cgrav.cpt -P -K > \$ps
5	Map elements (grid, title, coastline, title)	gmt pscoast -R -J -P -V -W0.25p -Df -B+"Marine free-air gravity anomaly: New Britain and San Cristobal trenches area" -Bxa4g3f2 -Bya4g3f2 -O -K >> \$ps
6	Adding scale and directional rose	gmt psbasemap -R -J -Tdg143/58.5+w0.5c+f2+l -Lx13.5c/1.3c+c50+w500k+"Mercator projection. Scale, km"+f -UBL/-5p/-40p -O -K >> \$ps
7	Adding legend	gmt psscale -R -J -Cgrav.cpt -Dg136.5 -15+w11.0c/0.5c+v+o0.7/0i+m1 -Baf+l"Marine free-air gravity anomaly color scale" -I0.2 -By+lmGal -O -K >> \$ps
8	Adding logo	gmt logo -R -J -Dx6.5/-2.2+o0.1i/0.1i+w2c -O -K >> \$ps
9	Adding subtitle	gmt pstext -R0/10/0/15 -JX10/10 -X0.5c -Y1.8c -N -O -F+f10p,Palatino-Roman,black+jLB >> \$ps << EOF 3.0 15.0 Global gravity grid from CryoSat-2 and Jason-1, 1 min resolution EOF
10	Converting to jpg by GhostScript	gmt psconvert Grav_NBT.ps -A0.2c -E720 -Tj -P -Z

Source: Author (2020).

The map resulting from this sequence of GMT codes in 10 steps is presented on Fig. 4. The accuracy of the marine gravity measurements is crucial for the data modelling (WESSEL; WATTS, 1988). Therefore, modelling free-air gravity model was done using data from high quality grids for gravity anomaly model from the Scripps Institute of Oceanography from CryoSat-2 and Jason-1 (SANDWELL et al., 2014). The fundamental approach of the marine gravity field modelling is described by SMITH and SANDWELL (1995). The free-air gravity map (Fig. 4) illustrates values (mGal) of the density anomalies at bathymetry, sediments, crust and mantle in the region of the trenches. The free-air

anomaly is dominated by the short wavelength variations which reflect the density contrast at the seafloor.

Digitizing cross-section profiles for relief modelling

Cartographic digitizing process differ for various GIS. In manual digitizing normal steps include map referencing, manual digitizing, node snapping, topology building, labelling of the resulting object. However, the methodology, in in general tedious and laborious. To make the process of digitizing easier and more precise, attempts in automatization and machine learning algorithms were introduced (SCHENKE; LEMENKOVA, 2008). The GMT proposed further advances in batch processing through scripting approach with a case of hill elevations (WESSEL and SMITH, 2018), used and adapted in this study.

Here, the inverse research task has been solved, that is, modelling hadal trench illustrated on Fig. 5. The 'grdtrack' module of GMT was used to sample the SRTM grid along the cross profiles in two trenches. The 'grdtrack' module algorithm enabled to do cross-sectioning by reading grid files and a table with (lon, lat) positions in the first two columns. A digitized trace used as a starting and ending points along which a segment was plotted (Fig. 5). Then the tracing was done automatically with a set up parameters (400 km long, space 20 km, sample every 2 km). Then the GMT interpolated the grid at the positions in the table and wrote the output table with the interpolated values (depths in km) added as new columns of the file. The algorithm was repeated for the 2nd trench. This is the core methodology of the automated digitizing cross-section profiles by GMT. As a result, GMT created a series of the orthogonal cross-profiles at each data point where it crossed the two trenches. The produced profiles are illustrated on Fig. 6. The coding algorithm is as follows (Table 2):

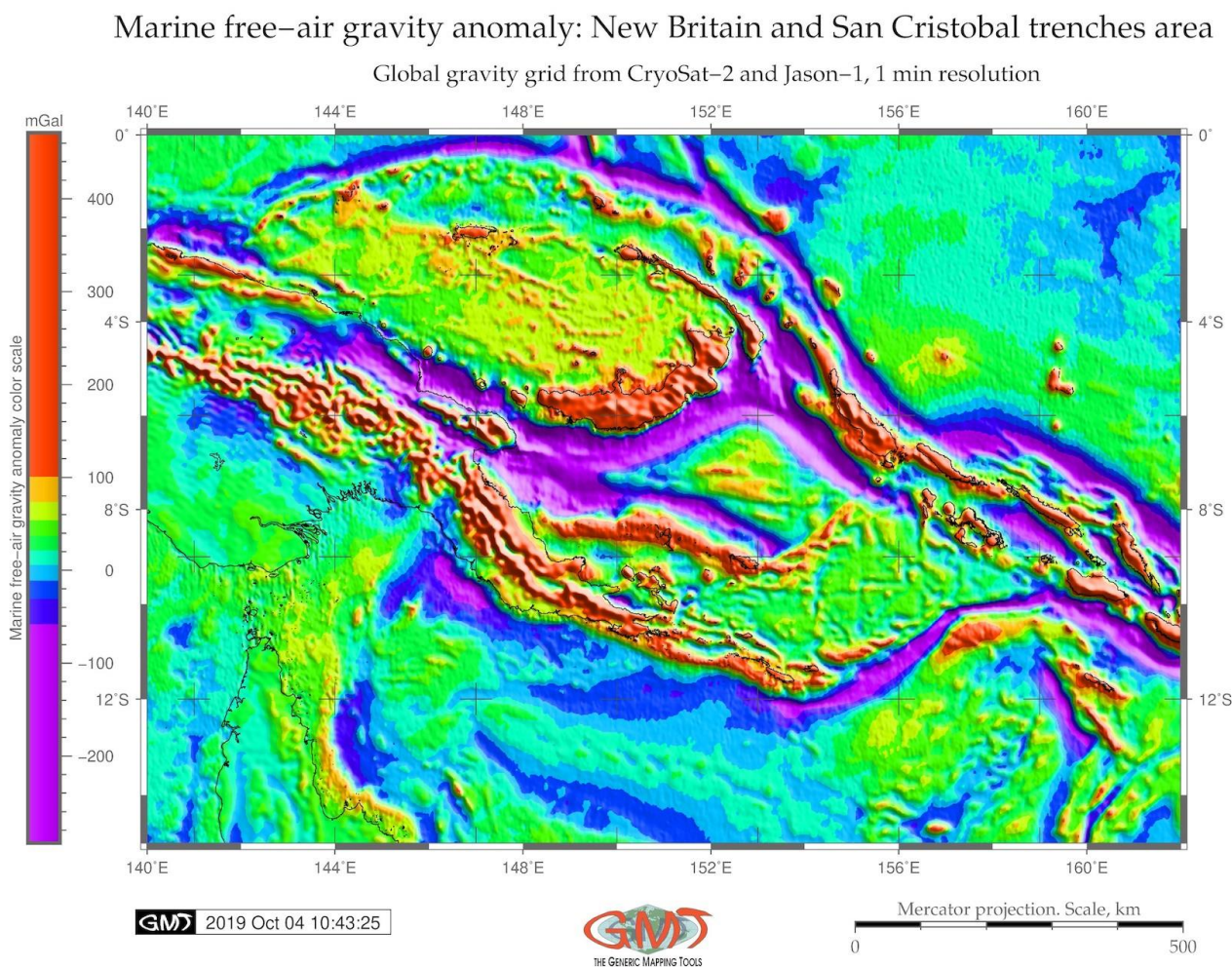
Table 2: Sequence of codes by GMT modules for cross-section profiles.

Step	Purpose of code	GMT code using various modules
1	Select two points along the segment	cat << EOF >
2	Plotting the line	trenchSCT.txt 153.5 -6.1 155.0 -7.4 EOF
3	Visualizing start and end points	gmt psxy -Rnbts_relief.nc -J -W2p,red trenchSCT.txt -O -K >> \$ps gmt psxy -R -J -Sc0.15i -Gred trenchSCT.txt -O -K >> \$ps
4	Cross-track profiles	gmt grdtrack trenchSCT.txt -Gnbts_relief.nc -C400k/2k/20k -Sm+sstackSCT.txt > tableSCT.txt
5	Plotting the profiles	gmt psxy -R -J -Wthin,red tableSCT.txt -O -K >> \$ps
6	Show upper/lower values encountered as an envelope	gmt convert stackSCT.txt -o0,5 > envSCT.txt gmt convert stackSCT.txt -o0,6 -l -T >> envSCT.txt

Source: author.

The map resulting from this sequence of GMT codes in 6 steps is presented on Fig. 5. A case is given for San Cristobal segment (red). The geometrical characteristics of both trench segments were determined with respect to bathymetry: since the San Cristobal Trench is longer, the comparative transect located closer to the New Britain Trench was selected for modelling. The selected positions of the starting and ending points of the segments are indicated on Fig. 5 shows the trench axes in a direction perpendicular to the transect. The bathymetric modeled data is SRTM DEMs. 14 profiles were cross-sectioned for the New Britain Trench and 12 profiles for the San Cristobal Trench.

Figure 4: Marine free-air gravity anomaly in the region of New Britain and San Cristobal trenches.



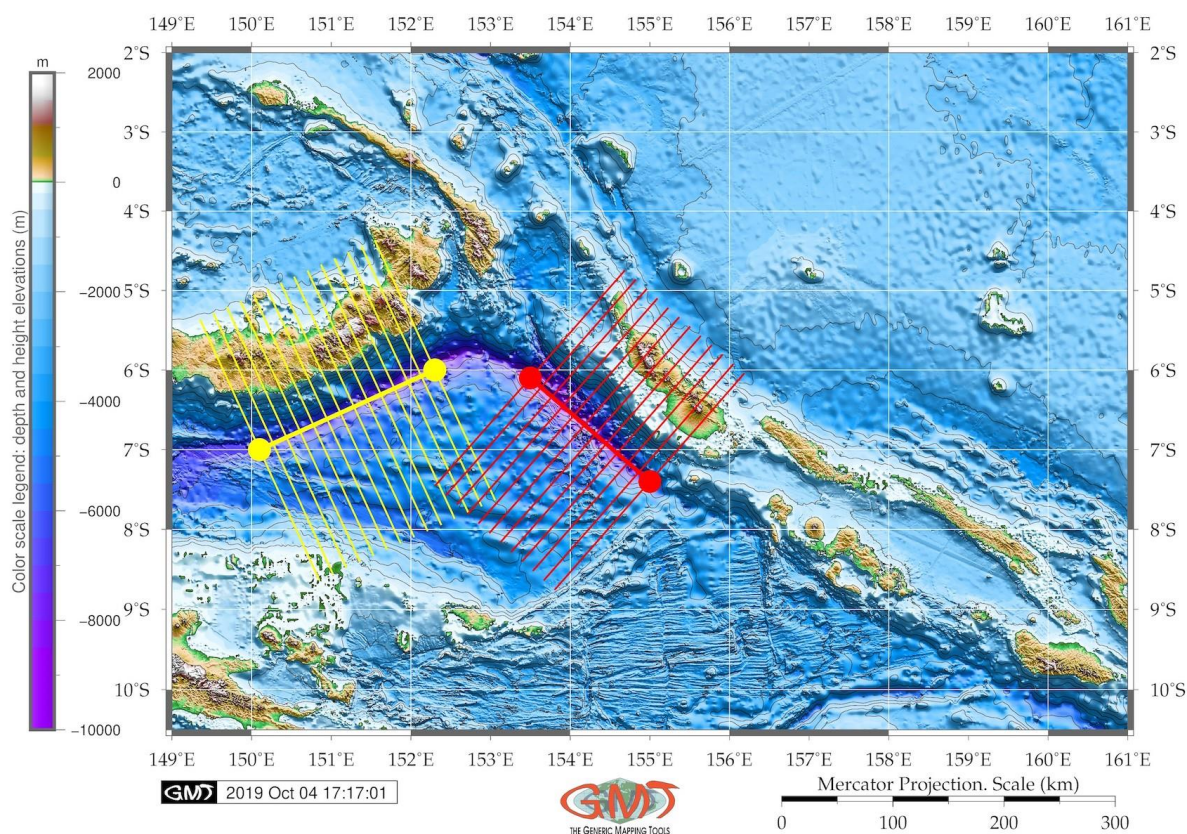
Source: Author (2020).

The comparative analysis of the two trenches was done through modelling their relief at cross-sections (Fig. 6), followed by statistical calculations of the depths and visualizing their histograms (Fig. 7) and then plotting approximating curves of the gradient slopes for two trenches, respectively (Fig. 8).

The New Britain Trench is shallower compared to the San Cristobal Trench: it has median values not exceeding -7,000m (vs -8,000 m median value for the San Cristobal). The New Britain Trench has more asymmetrical U-shaped cross-section dipping westwards with 35° eastward slope, and 41° westward slope (Fig. 6 A). The San Cristobal Trench has 33° slope oceanwards while 33,69° landwards increasing in relief more direct on the oceanward side. The increase in depth by New Britain Trench is more gentle: in 50km segment it reaches 2000 m depths (from -7,000 to -5,000) while the increase for the San Cristobal Trench is more abrupt: for the same distance (50 km) the depths rise from -8,000 to -5,200 m (that is, almost 3000 m), Fig. 6. Associated to the oceanward side of the San Cristobal Trench, several separated minor canyons and furrows has been defined (Fig. 6, A), while New Britain Trench has gentle slope on the Solomon Sea side. In the cross-section graph, the New Britain Trench is markedly asymmetric in the landward slope and has an arc form in the east (Fig. 6, B).

Figure 5: Digitized profiles of the New Britain and San Cristobal trenches.

Cross-sectional profiles on two selected segments of trenches: New Britain (yellow) and San Cristobal (red)



Source: Author (2020).

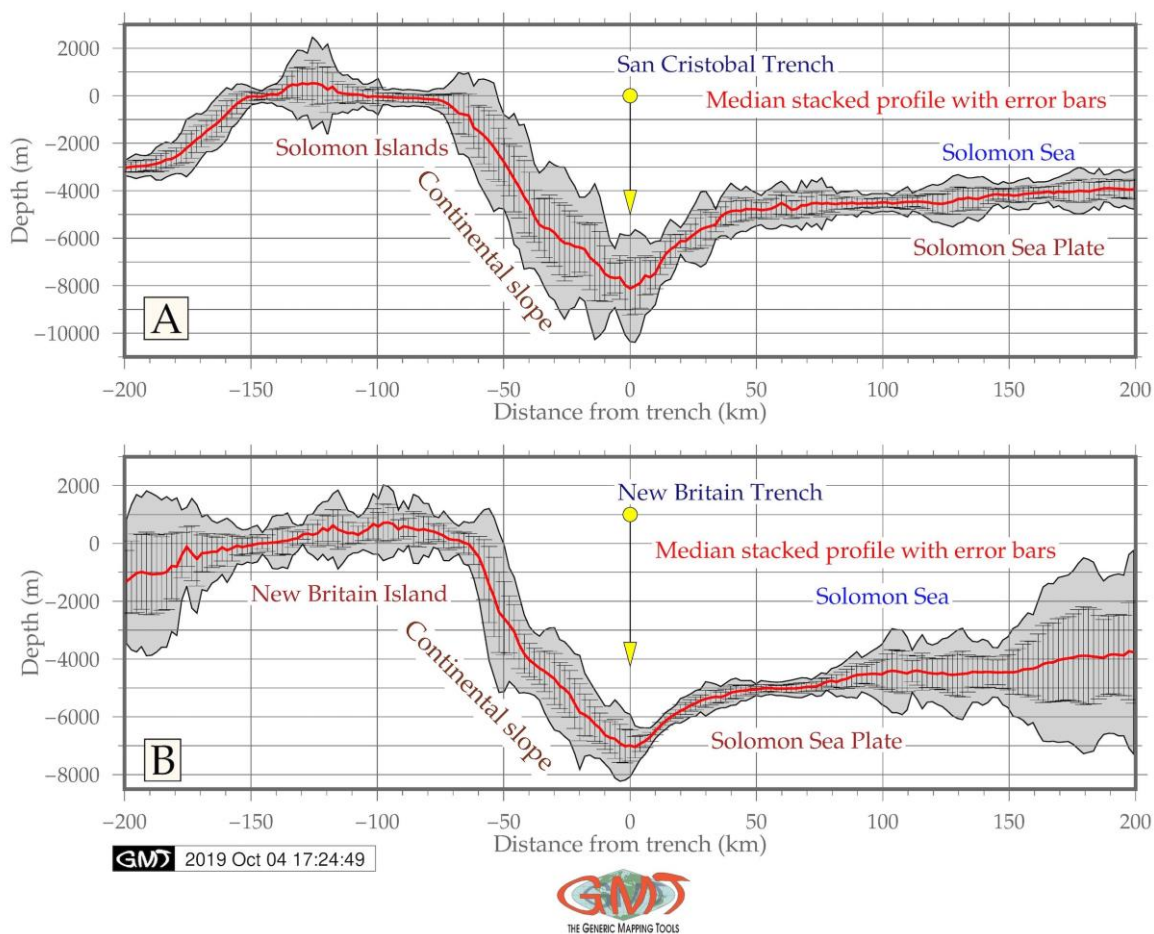
The San Cristobal Trench is more symmetric having accurate 'V' form for the segment of -50 to -50 km on the graph (Fig. 6, A). The depth to the bottom of the New Britain Trench becomes gradually

deeper in a segment of -50 to 0 m in cross-section, decreasing from -3,000 to -7,000 in WE direction, with maximum depths reaching -7,000 m. For the same transect (segment of -50 to 0 m in a cross-section) for the San Cristobal Trench, the depth to the bottom becomes deeper decreasing from -3,000 to -8,000 in WE direction, that is, the gradient slope is steeper. The differences between the two trenches are explained by the context of the historic and actual geomorphic and sedimentary processes that finally affected their formation and structure.

RESULTS

The main resulting modeled graphs of the profiles of the two deep-sea trenches are visualized in Fig. 6. The statistical comparison of the two trenches (Fig. 7) shows that the San Cristobal is generally deeper with bathymetric data reaching -9,000 meters while New Britain Trench has only 1 sample point below -8,000 m.

Figure 6: Graphs of the relief models of the New Britain and San Cristobal trenches.

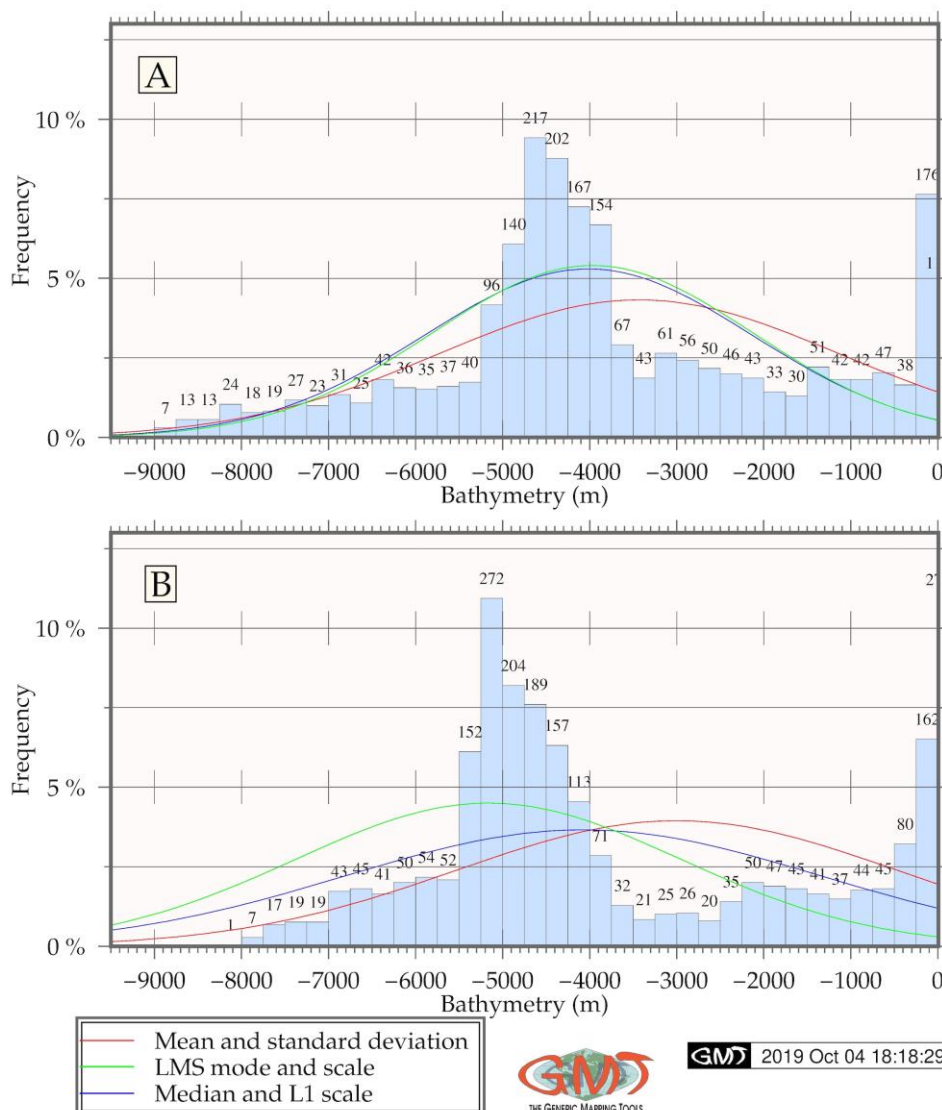


Source: Author (2020).

The most frequent values for the San Cristobal Trench lie in range from -4,600 to -4,800 m (217 samples), -4,600 to -4,400 (202 samples) and -4,400 to -4,200 (167 samples). As for the New Britain Trench, the highest values of the observation samples are recorded in range -5,000 to -5,200 m (272) gradually followed by ranges -5,200 to -5,000, -5,000 to -4,800 and -4,800 to -4,600 m (number of samples recorded: 204, 189, 157). That is, the histogram for the New Britain Trench has a slightly more skewed truncated view (right-sided) with visually dominating values in shallower depths, while diminishing values below -5,000 m b.s.l. comparing to the San Cristobal Trench with bell-shaped normal data distribution. The majority of the observation samples for both trenches lie in range of -4000 to -5,000 m.

Figure 7: Histograms of the bathymetry in New Britain and San Cristobal trenches.

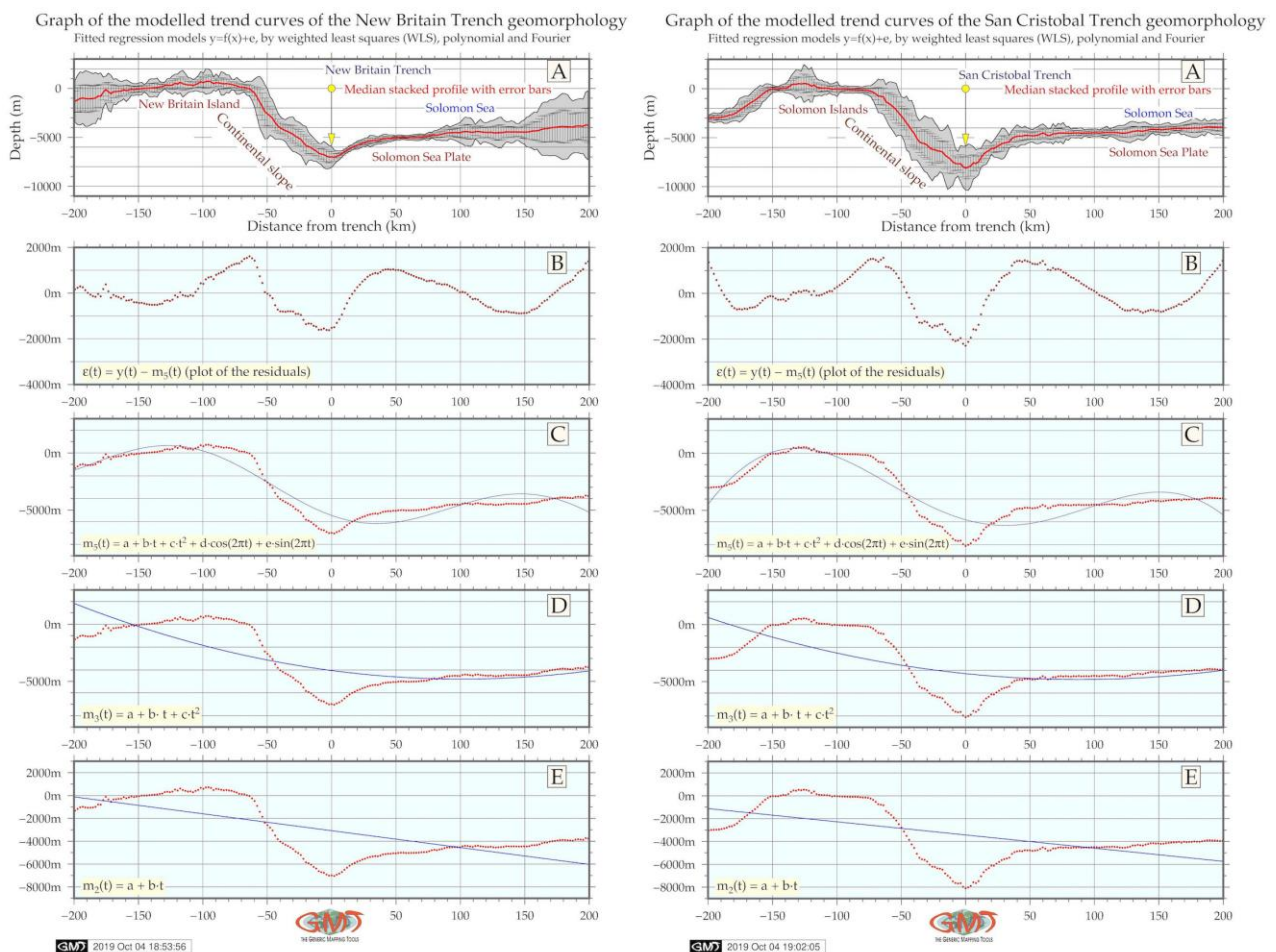
Histograms of the bathymetry, San Cristobal (A) and New Britain (B) trenches



Source: Author (2020).

Mathematic approximation of the gradient slopes for both trenches is shown on Fig. 8 with applied 3 types of the Fourier functions modelling the general trend of the profile curves (median) and residuals plotted for both trenches. The free-air gravity anomalies (Fig. 4) derived from the satellite altimeter measured sea surface height (SSH) have an anomaly range from -60.0 mGal and lower over the hadal trenches (deep purple colour). The geoid shows density of the topographic structures and the upper mantle lithosphere, the geoid anomaly or height can be high irrespective of the real topography. Therefore, as can be seen (Fig. 3), the colour of geoid for the Papua New Guinea Island has similar range (65-85 mGal) as Bismarck Sea (orange colour on the map). The New Britain and San Cristobal Trenches are distinguishable by the isolines. Lower geoid values (42-65 mGal, lime colour) are notable for the regions north-east off the Solomon Islands. The tectonic and bathymetric complexity of the area (linear features, isolated constructs on the seafloor, seamounts) explains variations in the topographic patterns of the trenches.

Figure 8: Approximated trend curve models of the gradient slopes: New Britain Trench and San Cristobal Trench.



Source: Author (2020).

CONCLUSION

Understanding structure of the trench geomorphology is crucial for modelling Earth's seafloor, as trench may be located on the place of junction of several tectonic plates (LEMENKOVA, 2020f). The global plate tectonics movements shaping the seafloor bathymetry is one of the most challenging issues of solid Earth science. Broadly-speaking, the shape and present form of the hadal trenches are dominated by variations in set of geophysical and geological factors. Amongst them, the most fundamental is subducting slab morphologies in the deep mantle inducing trench formation (LEMENKOVA, P. 2018c).

Due to the rapidly developing computer technologies, precise modelling of the Earth became possible through data analysis and modelling. There are various approaches trying to find best and effective solutions in data processing and visualization in geoscience. Multiple examples of using statistical libraries and packages of R or Python languages exist for data analysis in Earth and general sciences (CHAMBERS, 2008; LEMENKOVA, 2019c; SARKAR, 2008; SKØIEN et al., 2014; BIVAND et al., 2013; LEMENKOVA, 2020b; HOFER; PAPRITZ, 2011; LEMENKOVA, 2020b). A vast variety of the examples of the geospatial mapping is supported by using traditional GIS (e.g., KLAUČO, et al. 2017; LEMENKOVA et al. 2012; KLAUČO et al., 2014). The examples of the bathymetric mapping, seafloor cartographic modelling and marine research (SUETOVA et al., 2005a; KUHN et al., 2006; SUETOVA et al., 2005b, LEMENKOVA, 2011) mostly use ArcGIS as a main tool for data analysis or its combination with CARIS HIPS and GMT (GAUGER et al. 2007).

Statistical analysis and processing of the oceanological and marine geological data can be performed by various approaches, such as regression models to visualize correlation between geological variables (CHILÉS and DELFINER, 1999; LEMENKOVA, 2019d), geodata clustering and grouping, modelling and visualizing, sorting and comparing by various statistical approaches (LEMENKOVA, 2019e; CRESSIE, 1991; KLAUČO et al. 2013a, 2013b; LINDH, 2004), cartographic mapping (LEMENKOVA, 2020c, 2020d, 2020e), kriging for the geodata interpolation (SKØIEN et al., 2006).

Comparing to the vast variety of approaches in data analysis, briefly mentioned above, with the methodology and results demonstrated in this paper, what seems to be advantageous in using GMT? There are several answers to this question. First, the high cartographic level of the GMT functionality, as demonstrated on the maps presented in this paper: high quality cartographic solutions, colour palettes, projections, layout, data visualization. Second, the flexibility of the GMT coding and shell scripting.

Third, the compatibility of the GMT with UNIX environment. Fourth, the flexibility of GMT that enables to do all kind of data analysis and visualization: cartographic mapping, graphical modelling,

data queries and logical questions, statistical analysis, data import/export, processing of both vector layers and raster grids. Fifth and last (but not least): the open source nature of the free-of-charge GMT over commercial GIS software is an evident advantage for students, researchers and general public.

CONFLICTS OF INTEREST

No conflicts of interest.

ACKNOWLEDGEMENT

The author would like to express the gratitude to the anonymous reviewers for the comments, corrections and remarks which improved the manuscript. This research was implemented into the framework of the project No. 0144-2019-0011, Schmidt Institute of Physics of the Earth, Russian Academy of Sciences.

REFERENCES

- ABBOTT, L. D.; SILVER, E. A.; GALEWSKY, J. Structural evolution of a modern arc–continent collision in Papua New Guinea. **Tectonics**, v. 13, p. 1007–1034, 1994.
- AUZENDE, J.-M.; GÉLI, L.; ONDRÉAS, H.; COLLOT, J.-Y.; LAFOY, Y.; EISSEN, J.-P.; GRACIA, E.; LARUE, M. B.; OLISUKULU, C.; TOLIA, D.; BILIKI, N. Evidence for sinistral strike-slip deformation in The Solomon Island arc. **Geo-Marine Letters**, v. 14, p. 232–237, 1994. <https://doi.org/10.1007/BF01274058>
- BALDWIN, S. L.; FITZGERALD, P. G.; WEBB, L. E. Tectonics of the New Guinea Region. **Annual Review of Earth and Planetary Sciences**, v. 40, p. 495–520, 2012. <https://doi.org/10.1146/annurev-earth-040809-152540>
- BECKER, J. J.; SANDWELL, D. T.; SMITH, W. H. F.; BRAUD, J.; BINDER, B.; DEPNER, J.; FABRE, D.; FACTOR, J.; INGALLS, S.; KIM, S.-H.; LADNER, R.; MARKS, K.; NELSON, S.; PHARAOH, A.; TRIMMER, R.; VON ROSENBERG, J.; WALLACE, G.; WEATHERALL, P. Global bathymetry and elevation data at 30 arc-seconds resolution: SRTM30 PLUS. **Marine Geodesy**, v. 32, p. 355–371, 2009. <https://doi.org/10.1080/01490410903297766>
- BIEDA, A.; BYDŁOSZ, J.; PARZYCH, P.; PUKANSKÁ, K.; WÓJCIAK, E. 3D Technologies as the Future of Spatial Planning: the Example of Krakow. **Geomatics and Environmental Engineering**, v. 14, n. 1, p. 15–33. 2020. <https://doi.org/10.7494/geom.2020.14.1.15>
- BIVAND, R. S.; PEBESMA, E.; GÓMEZ-RUBIO, V. **Applied Spatial Data Analysis with R, Use R**, 2nd ed., 10, Springer, New York, USA, 2013.
- CHAMBERS, J. M. **Software for Data Analysis Programming with R**. Springer, In: J. Chambers, J., Hand, D., & Härdle, W. (eds). Series: Statistics and Computing, 2008. <https://doi.org/10.1007/978-0-387-75936-4514>
- ČESNULEVIČIUS, A.; ŠUTINIENĖ, L.; KRIKŠČIŪNIENĖ, V.; SVILIENĖ, R.; MAČIULEVIČIŪTĖ-TURIENE, N.; BAUTRĖNAS, A.; BECONYTĖ, G.; OVODAS, D.; BEVAINIS, L. The structure of Volume III of the National Atlas of Lithuania and techniques of cartographic visualization. **Polish Cartographical Review**, v. 51, n. 1, p. 19–27, 2019. <https://doi.org/10.2478/pcr-2019-0003>
- CHILÉS, J.-P.; DELFINER, P. **Geostatistics. Modelling Spatial Uncertainty**. Wiley, New York, 1999.

- CRESSIE, N. **Statistics for Spatial Data**. Wiley-Interscience Publication, New York, NY, 1991.
- DAVIES, H. L.; KEENE, J.; HASHIMOTO, K.; JOSHIMA, M.; STUART, J.; TIFFIN, D. Bathymetry and canyons of the western Solomon Sea. **Geo-Marine Letters**, v. 6, p. 181–191, 1987. <https://doi.org/10.1007/BF02239579>
- DENT, B. **Cartography: thematic map design**. 5th ed. Boston: WCB/McGraw-Hill, 1999.
- FINLAYSON, D. M.; CULL, J. P. Structural profiles in New Britain-New Ireland region. **Journal of the Geological Society of Australia**, v. 20, p. 37–47, 1973.
- GAUGER, S.; KUHN, G.; FEIGL, T.; LEMENKOVA, P. Swath-bathymetric mapping. In: Gohl, K. The expedition ANTARKTIS-XXIII/4 of the Research Vessel 'Polarstern'. **Reports on Polar and Marine Research**, v. 557, p. 38-45, 2007. <https://doi.org/10.6084/m9.figshare.7439231>
- GESCH, D.; FARR, T.; SLATER, J.; MULLER, J.-P.; COOK, S. New products from the Shuttle Radar Topography Mission. **EOS Transactions of the AGU**, v. 87, p. 174, 2006. <https://doi.org/10.1029/2006EO180003>
- GESCH, D.; MULLER, J.-P.; FARR, T. G. The Shuttle Radar Topography Mission – Data validation and applications, foreword to special issue. **Photogrammetric Engineering and Remote Sensing**, v. 72, p. 233–234, 2006.
- GOMARASCA, M. A. Elements of Cartography. In: **Basics of Geomatics**. Springer, Dordrecht, 2009. https://doi.org/10.1007/978-1-4020-9014-1_2
- HOFER, C.; PAPRITZ, A. Constrained kriging: An R-package for customary, constrained and covariance-matching constrained point or block kriging. **Computers and Geosciences**, v. 37, n. 10, p. 1562–1569, 2011. <https://doi.org/10.1016/j.cageo.2011.02.009>
- HOLM, R. J.; TAPSTER, S.; JELSMA, H. A.; ROSENBAUM, G.; MARK, D. F. Tectonic evolution and copper-gold metallogenesis of the Papua New Guinea and Solomon Islands region. **Ore Geology Reviews**, v. 104, p. 208–226, 2019. <https://doi.org/10.1016/j.oregeorev.2018.11.007>
- HONZA, E.; DAVIES, H. L.; KEENE, J. B.; TIFFIN, D. L. Plate boundaries and evolution of the Solomon Sea region. **Geo-Marine Letters**, v. 7, p. 161–168, 1987. <https://doi.org/10.1007/BF02238046>
- JOHNSON, R. W. **Late Cainozoic volcanism and plate tectonics at the southern margin of the Bismarck Sea, Papua New Guinea**. In: *Volcanism in Australasia: A collection papers in honour of the late G.A.M. Taylor, G.C.*, Elsevier, Amsterdam, p. 101–116, 1976.
- KEATES, S. J. **Understanding maps**, 2nd ed. Longman, Essex, 1996.
- KESKIN, M.; OOMS, K.; DE MAEYER, P.; DOGRU, A. O. Design of a cartographic eye tracking-EEG user experiment. In: **29th International Cartographic Conference (ICC 2019)**, 15–20 July 2019, Tokyo, Japan, p. 1-2. <https://doi.org/10.5194/ica-abs-1-171-2019>
- KLAUČO, M.; GREGOROVÁ, B.; STANKOV, U.; MARKOVIĆ, V.; LEMENKOVA, P. Determination of ecological significance based on geostatistical assessment: a case study from the Slovak Natura 2000 protected area. **Open Geosciences**, v. 5, n. 1, p. 28–42, 2013a. <https://doi.org/10.2478/s13533-012-0120-0>
- KLAUČO, M.; GREGOROVÁ, B.; STANKOV, U.; MARKOVIĆ, V.; LEMENKOVA, P. Interpretation of Landscape Values, Typology and Quality Using Methods of Spatial Metrics for Ecological Planning". In: **Environmental & Climate Technologies**. Latvia, Riga, 2013. <https://doi.org/10.13140/RG.2.2.23026.96963>
- KLAUČO, M.; GREGOROVÁ, B.; STANKOV, U.; MARKOVIĆ, V.; LEMENKOVA, P. Landscape metrics as indicator for ecological significance: assessment of Sitno Natura 2000 sites, Slovakia. In: **Ecology and Environmental Protection**. Minsk, Belarus, 2014, 85-90. <https://doi.org/10.6084/m9.figshare.7434200>

KLAUČO, M.; GREGOROVÁ, B.; KOLEDA, P.; STANKOV, U.; MARKOVIĆ, V.; LEMENKOVA, P. Land planning as a support for sustainable development based on tourism: A case study of Slovak Rural Region. **Environmental Engineering and Management Journal**, v. 2, n. 16, p. 449–458, 2017. <https://doi.org/10.30638/eemj.2017.045>

KOCH, A.; HEIPKE C.; LOHMANN, P. Analysis of SRTM DTM methodology and practical results. In: **Symposium on geospatial theory, processing and applications, commission IV, WG IV/6**, Ottawa, 2002.

KUHN, G.; HASS, C.; KOBER, M.; PETITAT, M.; FEIGL, T.; HILLENBRAND, C. D.; KRUGER, S.; FORWICK, M.; GAUGER, S.; LEMENKOVA, P. The response of quaternary climatic cycles in the South-East Pacific: development of the opal belt and dynamics behavior of the West Antarctic ice sheet. In: **Expeditionsprogramm Nr. 75 ANT XXIII/4**, AWI, Bremerhaven, Germany, 2006. <https://doi.org/10.13140/RG.2.2.11468.87687>

KULP, S. A.; STRAUSS, B. H. CoastalDEM: A global coastal digital elevation model improved from SRTM using a neural network. **Remote Sensing of Environment**, v. 206, p. 231–239, 2018. <https://doi.org/10.1016/j.rse.2017.12.026>

LEMENKOVA, P. Seagrass Mapping and Monitoring Along the Coasts of Crete, Greece. M.Sc. Thesis. University of Twente, 2011. <https://doi.org/10.13140/RG.2.2.16945.22881>

LEMENKOVA, P.; PROMPER, C.; GLADE, T. Economic Assessment of Landslide Risk for the Waidhofen a.d. Ybbs Region, Alpine Foreland, Lower Austria. In: Eberhardt, E. et al. eds. Protecting Society through Improved Understanding. **11th International Symposium on Landslides and the 2nd North American Symposium on Landslides and Engineered Slopes (NASL)**, Banff, Canada, June 2–8 2012, p. 279–285. <https://doi.org/10.6084/m9.figshare.7434230>

LEMENKOVA, P. R scripting libraries for comparative analysis of the correlation methods to identify factors affecting Mariana Trench formation. **Journal of Marine Technology and Environment**, v. 2, p. 35–42, 2018a. <https://doi.org/10.6084/m9.figshare.7434167>

LEMENKOVA, P. Factor Analysis by R Programming to Assess Variability Among Environmental Determinants of the Mariana Trench. **Turkish Journal of Maritime and Marine Sciences**, v. 4, p. 146–155, 2018b. <https://doi.org/10.6084/m9.figshare.7358207>

LEMENKOVA, P. Geomorphological modelling and mapping of the Peru-Chile Trench by GMT. **Polish Cartographical Review**, v. 51, n. 4, p. 181–194, 2019a. <https://doi.org/10.2478/pcr-2019-0015>

LEMENKOVA, P. Automatic Data Processing for Visualising Yap and Palau Trenches by Generic Mapping Tools. **Cartographic Letters**, v. 27, n. 2, p. 72–89, 2019b. <https://doi.org/10.6084/m9.figshare.11544048>

LEMENKOVA, P. Statistical Analysis of the Mariana Trench Geomorphology Using R Programming Language. **Geodesy and Cartography**, v. 45, n. 2, p. 57–84, 2019c. <https://doi.org/10.3846/gac.2019.3785>

LEMENKOVA, P. Topographic surface modelling using raster grid datasets by GMT: example of the Kuril-Kamchatka Trench, Pacific Ocean. **Reports on Geodesy and Geoinformatics**, v. 108, p. 9–22, 2019d. <https://doi.org/10.2478/rgg-2019-0008>

LEMENKOVA, P. GMT Based Comparative Analysis and Geomorphological Mapping of the Kermadec and Tonga Trenches, Southwest Pacific Ocean. **Geographia Technica**, v. 14, n. 2, p. 39–48, 2019e. https://doi.org/10.21163/GT_2019.142.04

LEMENKOVA, P. SAGA GIS for information extraction on presence and conditions of vegetation of northern coast of Iceland based on the Landsat TM. **Acta Biologica Marisiensis**, v. 3, n. 2, p.10-21, 2020a. <https://doi.org/10.2478/abmj-2020-0007>

LEMENKOVA, P. R Libraries {dendextend} and {magrittr} and Clustering Package scipy.cluster of Python For Modelling Diagrams of Dendrogram Trees. **Carpathian Journal of Electronic and Computer Engineering**, v. 13, n. 1, p. 5–12, 2020b. <https://doi.org/10.2478/cjece-2020-0002>

- LEMENKOVA, P. Variations in the bathymetry and bottom morphology of the Izu-Bonin Trench modelled by GMT. **Bulletin of Geography. Physical Geography Series**, v. 18, n. 1, p. 41–60, 2020c. <https://doi.org/10.2478/bgeo-2020-0004>
- LEMENKOVA, P. Fractal surfaces of synthetical DEM generated by GRASS GIS module r.surf.fractal from ETOPO1 raster grid. **Journal of Geodesy and Geoinformation**, v. 7, n. 1, p. 86–102, 2020d. <https://doi.org/10.9733/JGG.2020R0006.E>
- LEMENKOVA, P. GEBCO Gridded Bathymetric Datasets for Mapping Japan Trench Geomorphology by Means of GMT Scripting Toolset. **Geodesy and Cartography**, v. 46, n. 3, p. 98–112, 2020e. <https://doi.org/10.3846/gac.2020.11524>
- LEMENKOVA, P. GMT Based Comparative Geomorphological Analysis of the Vityaz and Vanuatu Trenches, Fiji Basin. **Geodetski List**, v. 74, n. 1, p. 19–39, 2020f. <https://doi.org/10.6084/m9.figshare.12249773>
- LINDH P. **Compaction- and strength properties of stabilised and unstabilised fine-grained tills**. PhD Thesis, Lund University, Lund, 2004.
- LINDLEY, I. D. New Britain Trench, Papua New Guinea: An extensional element in a regional sinistral strike-slip system. **New Concepts in Global Tectonics Newsletter**, v. 41, p. 15-27, 2006.
- LINDLEY, I. D. Early Cainozoic stratigraphy and structure of the Gazelle Peninsula, east New Britain: An example of extensional tectonics in the New Britain arc-trench complex. **Australian Journal of Earth Sciences**, v. 35, p. 231–244, 1988. <https://doi.org/10.1080/14400958808527943>
- LÓPEZ, F. J. A.; BALBOA, J. L. G. Approximating Cartography to the Customer's Expectations: Applying the „House of Quality“ to Map Design. **Cartographica**, v. 43, p. 107–123, 2008. <https://doi.org/10.3138/cart.43.2.107>
- MACEACHREN, A. M. **How maps work: Representation, Visualization & Design**. Guilford Publications, New York, 1995.
- MAMMERICKX, J.; CHASE, T. E.; SMITH, S. M.; TAYLOR, I. L. **Bathymetry of the South Pacific. Chart 11**. Scripps Institute of Oceanography and Institute of Marine Science, La Jolla, 1971.
- MESENBUR, G. P. Abbildungen gestern und heute – Die Weltkarte des Gerhard Mercator aus dem Jahre 1569. In: **Kartographische Schriften**, Kirschbaum Verlag, Bonn. 9, 186–195, 2004.
- OSTROWSKI, W.; DUKACZEWSKI, D.; MARKOWSKA, A. Presentation of build-up areas on topographic maps of selected European countries. **Polish Cartographical Review**, v. 51, n. 1, p. 1–14, 2019. <https://doi.org/10.2478/pcr-2019-0001>
- PHAM, H. T.; MARSHALL, L.; JOHNSON, F.; SHARMA, A. A method for combining SRTM DEM and ASTER GDEM2 to improve topography estimation in regions without reference data. **Remote Sensing of Environment**, v. 210, p. 229–241, 2018. <https://doi.org/10.1016/j.rse.2018.03.026>
- RIPPER, I. D. (1970). Global tectonics and the New Guinea-Solomon Islands region. **Search**, v. 1, p. 226–232.
- ROBINSON, A. H.; MORRISON, J. L.; MUEHRCKE, P. C.; KIMERLING, A. J.; GUPTILL, S. C. **Elements of cartography**. 6th ed. New York: Wiley, 1995.
- SANDWELL, D. T.; MÜLLER, R. D.; SMITH, W. H. F.; GARCIA, E.; FRANCIS, R. New global marine gravity model from CryoSat-2 and Jason-1 reveals buried tectonic structure. **Science**, v. 346, n. 6205, p. 65–67, 2014. <https://doi.org/10.1126/science.1258213>
- SARKAR, D. **Lattice: Multivariate Data Visualization with R**. Springer, 2008. <https://doi.org/10.1007/978-0-387-75969-2>
- SCHENKE, H. W.; LEMENKOVA, P. Zur Frage der Meeresboden-Kartographie: Die Nutzung von AutoTrace Digitizer für die Vektorisierung der Bathymetrischen Daten in der Petschora-See. **Hydrographische Nachrichten**, v. 81, p. 16-21, 2008. <https://doi.org/10.6084/m9.figshare.7435538>

- SKØIEN, J. O.; BLÖSCHL, G.; LAAHA, G.; PEBESMA, E.; PARAJKA, J.; VIGLIONE, A. rtop: An R package for interpolation of data with a variable spatial support, with an example from river networks. **Computers & Geosciences**, v. 67, p. 180–190, 2014. <https://doi.org/10.1016/j.cageo.2014.02.009>
- SKØIEN, J. O.; MERZ, R.; BLÖSCHL, G. Top-kriging-geostatistics on stream networks. **Hydrology and Earth System Sciences**, v. 10, p. 277–287, 2006. <https://doi.org/10.5194/hess-10-277-2006>
- SLOCUM, T.; MCMASTER, R. B.; KESSLER, F. C.; HOWARD, H. H. **Thematic Cartography and Geovisualization**. 3rd ed: Prentice Hall, 2009.
- SMITH, W. H. F.; SANDWELL, D. T. Marine gravity field from declassified Geosat and ERS-1 altimetry. **EOS Transactions of the AGU**, 76, Fall Mtng Suppl, F156, 1995.
- SMITH, W. H. F. (1993). On the accuracy of digital bathymetric data. *Journal of Geophysical Research*, 98(B6), 9591–9603. <https://doi.org/10.1029/93JB00716>
- SUETOVA, I. A.; USHAKOVA, L. A.; LEMENKOVA, P. Geoinformation mapping of the Barents and Pechora Seas. **Geography and Natural Resources**, v. 4, p. 138–142, 2005. <https://doi.org/10.6084/m9.figshare.7435535>
- SUETOVA, I., USHAKOVA, L.; LEMENKOVA, P. Geocological Mapping of the Barents Sea Using GIS. In: **International Cartographic Conference ICC**. La Coruña, España, July 9–16 2005. <https://doi.org/10.6084/m9.figshare.7435529>
- TAYLOR, B. Bismarck Sea: evolution of a back-arc basin. **Geology**, v. 7, p. 171–174, 1979.
- TOBLER, W. R. **A Computer Program To Draw Perspective Views of Geographical Data**. University of Michigan, 5 p., 1974.
- TYNER, J. **Introductory to Thematic Cartography**, Prentice Hall, London, 299 p., 1992.
- TREGONING, P.; LAMBECK, K.; STOLZ, A.; MORGAN, P.; MCCLUSKY, S. C.; VAN DER BEEK, P.; MCQUEEN, H.; JACKSON, R. J.; LITTLE, R. P.; LAING, A.; MURPHY, B. Estimation of current plate motions in Papua New Guinea from Global Positioning System observations. **Journal of Geophysical Research**, v. 103, p. 181–203, 1998. <https://doi.org/10.1029/97JB03676>
- YOELI, P. Digital Terrain Models and their Cartographic and Cartometric Utilisation. **The Cartographic Journal**, v. 20, n.1, p. 17–22, 1983.
- WIEBENGA, W. A. **Crustal Structure of the New Britain-New Ireland Region**. In: Coleman, P.J. (ed.) Proceedings of a congress, Canberra, Australia, Aug. 1971. Patick J. Coleman, Ed. Crane, Russak, New York, and University of Western Australia Press, Nedlands, 1973. xviii, 676 pp., 163–177. <https://doi.org/10.1126/science.184.4137.688>
- WESSEL, P.; WATTS, A. B. On the accuracy of marine gravity measurements. **Journal of Geophysical Research**, 93, 393–413, 1988. <https://doi.org/10.1029/JB093iB01p00393>
- WESSEL, P.; SMITH, W. H. F. New, improved version of the generic mapping tools released. **EOS Transactions American Geophysical Union**, v. 79, n. 579, 1998. <https://doi.org/10.1029/98EO00426>
- WESSEL, P.; SMITH, W. H. F. A Global Self-consistent, Hierarchical, High-resolution Shoreline Database. **Journal of Geophysical Research**, v. 101, p. 8741–8743, 1996. <https://doi.org/10.1029/96JB00104>
- WESSEL, P.; SMITH, W. H. F.; SCHARROO, R.; LUIS, J.; WOBBE, F. Generic mapping tools: improved version released. **EOS Transactions AGU**, v. 94, n. 45, p. 409–410, 2013. <https://doi.org/10.1002/2013EO450001>
- WESSEL, P.; SMITH, W. H. F. **The Generic Mapping Tools. Version 4.5.18 Technical Reference and Cookbook** [Computer software manual]. U.S.A., 2018.

- WOOD, D. Maps and Mapmaking. **Cartographica**, v. 30, p. 1–9, 1993. <https://doi.org/10.3138/V167-G2U7-7356-6402>
- YANG, G.; SHEN, C.; WANG, J.; XUAN, S.; WU, G.; TAN, H. Isostatic anomaly characteristics and tectonism of the New Britain Trench and neighboring Papua New Guinea. **Geodesy and Geodynamics**, v. 9, n. 5, 404-410, 2018. <https://doi.org/10.1016/j.geog.2018.04.006>
- YONESHIMA, S.; MOCHIZUKI, K.; ARAKI, E.; HINO, R.; SHINOHARA, M.; SUYEHICO, K. Subduction of the Woodlark Basin at New Britain Trench, Solomon Islands region. **Tectonophysics**, v. 397, p. 225-239, 2005. <https://doi.org/10.1016/j.tecto.2004.12.008>
- ZHANG, K.; GANN, D.; ROSS, M.; ROBERTSON, Q.; SARMIENTO, J.; SANTANA, S.; RHOME, J.; FRITZ, C. Accuracy assessment of ASTER, SRTM, ALOS, and TDX DEMs for Hispaniola and implications for mapping vulnerability to coastal flooding. **Remote Sensing of Environment**, v. 225, p. 290-306, 2019. <https://doi.org/10.1016/j.rse.2019.02.028>